2006 IEEE International
Symposium on Signal Processing
and Information Technology

Effects of Mid-Sagittal Plane Perturbation and Image Interpolation on Corpus Callosum Area Calculation

Omer Ishaq[1], Ghassan Hamarneh[1], Roger Tam[2] and Anthony Traboulsee[2]
[1]Medical Image Analysis Lab, School of Computing Science, Simon Fraser University
8888 University Drive, Burnaby, BC V5A 1S6, Canada
[2]MS/MRI Research Group, Department of Medicine, University of British Columbia
Suite 211-2386 East Mall Vancouver, BC, V6T 1Z3, Canada

Abstract *— The corpus callosum (CC) is an anatomical structure that bridges the two brain hemispheres. It contains white matter tracts that participate in inter hemispheric communication. In multiple sclerosis (MS), the CC can have discrete lesions (MS plaques) or generalized tissue loss (atrophy), both of which affect the CC size. However, detection of changes in CC size depends on accurate identification of the mid-sagittal plane (MSP) in three dimensional space. We determine the error introduced in CC area when the plane of measurement is altered. Our contribution is the study of the effects of plane alteration and image interpolation. The interpolation techniques investigated are tricubic, trilinear and nearest neighbor. For measuring this error, we semi-automatically segment the CC in an MR volume. The voxels of the segmented volume are coded as binary values based on their position either inside or outside the CC. We then generate an MSP though reslicing and resampling of the volumetric data for varying values of MSP orientation and translation parameters. Finally we calculate the area of the CC whose cross section is embedded in the MSP.*

Keywords *— Medical image analysis, interpolation, corpus callosum, multiple sclerosis, mid sagittal plane, area calculation.*

I. Introduction

The CC and the MS are discussed in section I, section II focuses on the previous work, section III deals with the calculation of the introduced error in cross-sectional CC area due to MSP perturbation and image interpolation, sections IV and V provide the results and the conclusions, respectively.

A. Corpus Callosum

The CC is easily identified (figure 1(a)) in the mid-sagittal plane on magnetic resonance imaging (MRI). The CC connects the two brain hemispheres by acting as a bridge for the inter-hemispheric nerve fibers. The CC contains millions of nerve bundles transmitting nerve impulses between the hemispheres. A decrease in the cross-sectional area of the CC reflects a loss of the inter-hemispheric nerve fibers and consequently a decrease in the nerve impulses.

B. Multiple Sclerosis

Multiple Sclerosis is an auto-immune disease of the brain and the spinal cord (central nervous system) [5]. In MS, the immune system attacks the central nervous system causing inflammation and atrophy in the protective myelin covering around the nerves. The atrophy occurs in multiple patches in the central nervous system. In the CC, this atrophy can cause a disruption of nerve impulses along nerve fibers connecting the two brain hemispheres and a decrease in the cross-sectional area of the CC.

II. Previous Work

Previous work on studying the effects of MSP perturbation on CC area calculation does not take into consideration the effects of different image interpolation schemes on the error measurement [3, 9, 10, 11]. Our primary contribution is the study of the effects of both the MSP alteration and the image interpolation on the CC cross-sectional area. The interpolation techniques investigated are tricubic, trilinear and nearest neighbor. For measuring this error, we perform interactive semi-automatic segmentation of the CC located in the MR volumes. We chose to perform interactive semi-automatic segmentation rather than using fully automatic segmentation methods such as active appearance models [3, 14], active contour models [12, 15] or level set based methods [13, 16] because our selection of interactive semi-automatic segmentation ensures that the segmentations are guided and driven by human observers and that our measurements are free of errors introduced due to any inherent inaccuracy of the fully automatic segmentation algorithms. In [3] the CC cross-sections embedded in the MSP are segmented after each perturbation of the MSP whereas in our approach we initially segment the CC bridge in 10 sagittal slices for each MR volume and then perform the subsequent MSP perturbations without any further segmentations. This ensures that there is a smaller number of segmentations to be performed in our approach and due to this smaller number we can more easily perform expert verification of the correctness of the segmentations.

III. Methods

A. Reference Coordinate System

The reference coordinate system used for describing the MSP perturbations is based on the widely used Right-Anterior-Superior (RAS) [2] convention. We select the center of the human brain as the origin of the coordinate system (figure 1(b)), the positive X-axis extends from the origin towards the right direction, the positive Y-axis extends from the origin towards the anterior and the positive Z-axis extends from the origin towards the superior.

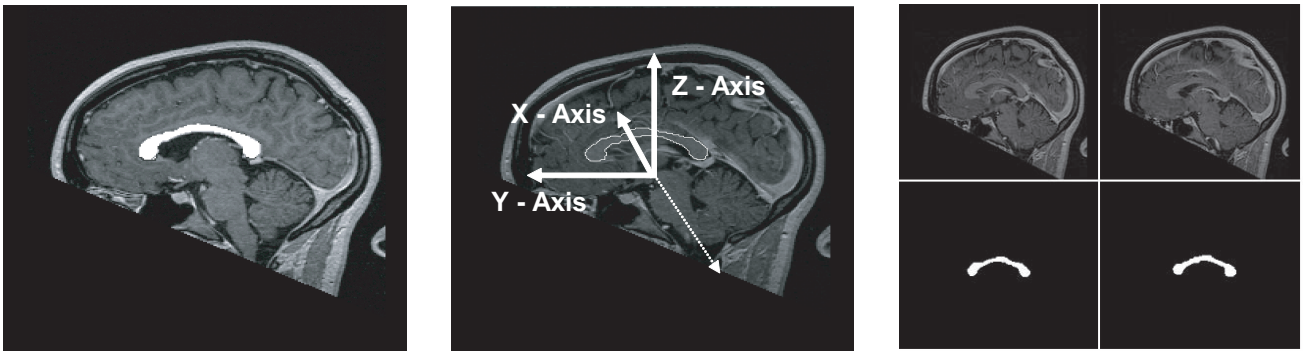

(a) CC in human brain

(b) RAS based reference coordinate system

(c) Segmented CC

Fig. 1. Demarcated Corpus Callosum in human brain

B. Data Transformations

Experiments for measurement of the effects of MSP alteration and image interpolation are performed on MR brain volumes of MS patients acquired using a 3D inversion-prepared spoiled gradient echo (SPGR) MRI sequence. Each volume is of dimensions $128 \times 256 \times 256$ voxels along the X,Y and Z axes. Each voxel has $1.25 \times 0.976 \times 0.976$ mm size along the three axes.

Since the acquired MR volumes have anisotropic voxel size, we perform super sampling of the MR volumes in order to obtain volumes with isotropic voxel size of $0.976 \times 0.976 \times 0.976$ mm, the super sampling changes the dimensions of each MR volume to $164 \times 256 \times 256$ voxels along the X,Y and Z axes. The super sampling is carried out using tricubic image interpolation. The choice of tricubic interpolation is due to its accuracy for reconstruction of medical images [7,8].

C. CC Segmentations

Semi-automatic segmentation of the CC in each MR volume is performed using Amira's Image Segmentation Editor (Mercury Computer Systems, Inc). The segmentation is performed only in the 10 center-most sagittal slices in each volume. Voxels inside and outside the segmented CC boundary are assigned binary image values 1 and 0, respectively (figure 1(c)).

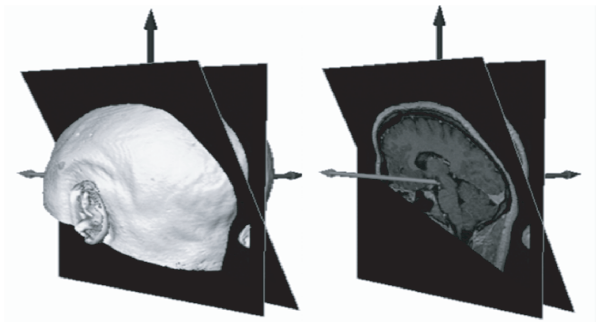

Fig. 2. MSP alteration through change of elevation

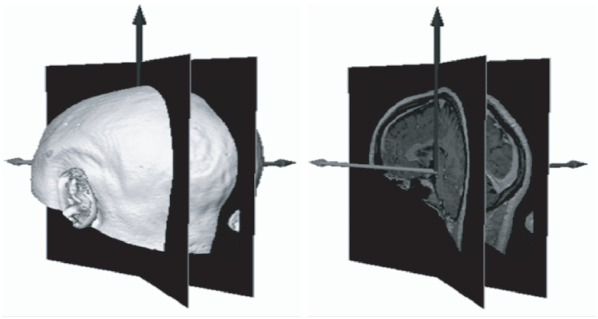

Fig. 3. MSP alteration through change of azimuth

D. Calculation of Effects of MSP Selection and Interpolation

The position of an MSP in an MR volume is dependent on its translation and orientation parameters. The translation of an MSP is defined as the position of the MSP from the origin along the X-axis. Orientation of an MSP is dependent on both the elevation and the azimuth angles of the MSP [3]. Changes in the elevation and the azimuth angles of an MSP are shown in figures 2 and 3, respectively. More specifically if an initial Y-Z plane is rotated around Y and Z axes, then, the elevation angle and the azimuth angle are the angles that the plane makes with the positive Z and Y axes, respectively. Therefore a 90 degree change in elevation angle converts a sagittal plane (Y-Z plane) into an axial plane (X-Y plane) whereas a 90 degree change in azimuth angle results in the conversion of a sagittal plane (Y-Z plane) to a coronal plane (X-Z plane).

For each MR volume the sagittal slice at slice position 82.5 in the 164 sagittal slice volume with 0 degree elevation and 0 degree azimuth is considered as the reference MSP because it is located in the center of the volume and therefore provides a convenient reference. It is also more likely to be in close

proximity of an anatomically correct MSP.

A set of perturbed MSPs relative to the reference MSP is generated through reslicing and resampling of the MR volume for given sets of values for the translation, elevation and azimuth parameters.

In our experiments, the translation range for the perturbed MSP is chosen to be the spacing of a single sagittal slice (0.976 mm) inclusive on both sides of the reference MSP with a step size equal to one half of the sagittal slice spacing (0.488 mm). We chose this translation range because it lies in the center of an MR volume and the CC has a well defined shape and boundary in this range. Choosing a smaller step size of 0.097 mm (0.1 sagittal slice spacing) or 0.195 mm (0.2 sagittal slice spacing) is possible. However this will result in a larger number of samples in our selected translation range, thus increasing the computations and running time of our experiment.

The range for both the elevation angle and the azimuth angle was chosen from -2.0 to 2.0 degrees inclusive with a step size of 0.2 degrees. We perform our experiments with a full factorial design and for each MR volume we have 5 different translation values, 21 different elevation values and 21 different values for the azimuth. This generates $5 \times 21 \times 21$ or 2205 unique perturbed MSPs for each MR volume.

These perturbed MSPs may not lie at the sampled data points in the MR volumes, therefore image interpolation is performed to obtain the image intensities at different MSP positions, The interpolation techniques used are tricubic, trilinear and nearest neighbor. The use of three different interpolation techniques for each of the 2205 perturbed MSP positions results in 2205×3 or 6615 MSPs.

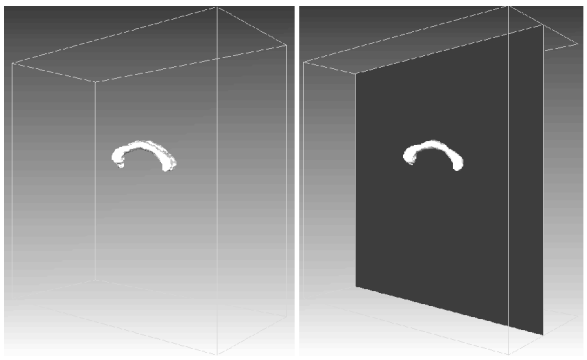

Fig. 4. (Left) Binary MR volume of the human brain, the segmented CC has intensity 1 and is shown in this figure by an iso-surface where as the rest of the human brain has intensity 0 and is shown as transparent. (Right) A mid sagittal plane passing through the CC bridge.

E. CC Area Calculation

Although the segmented data volumes were binary but the image intensities at the MSPs are no longer strictly binary due to image interpolation. The cross sectional area of the CC embedded in each of the MSPs is calculated by summation of the image intensities for each MSP and multiplication with the pixel resolution.

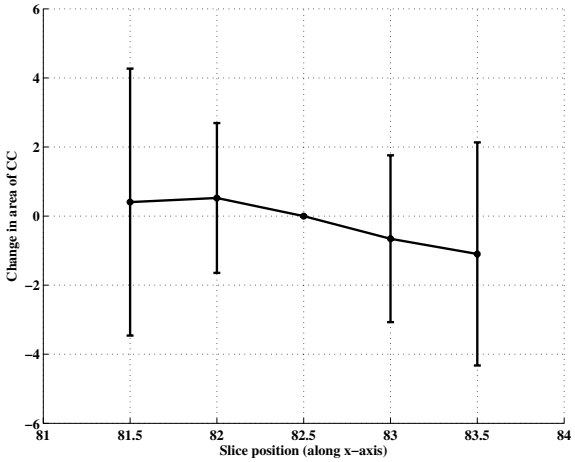

Fig. 5. Mean and standard deviation of percentage change (%) in CC area across the 15 MR volumes for tricubic interpolation plotted against change in translation

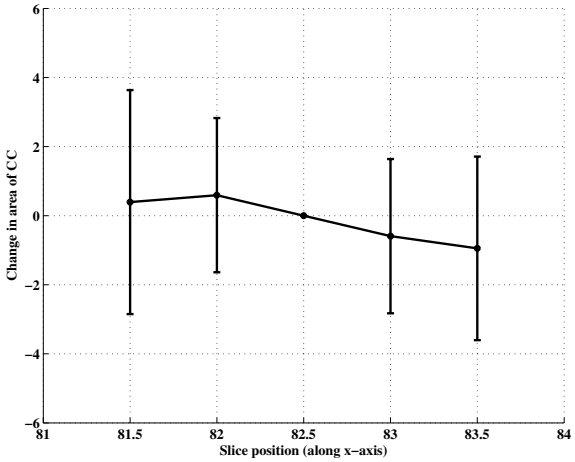

Fig. 6. Mean and standard deviation of percentage change (%) in CC area across the 15 MR volumes for trilinear interpolation plotted against change in translation

IV. RESULTS

MSP generation and CC area calculation was carried out for 15 MR brain volumes of 5 MS patients with 3 scans for each patient. For each volume, the cross-sectional area of the CC embedded in the reference MSP (sagittal slice position 82.5, 0 degrees elevation angle and 0 degrees azimuth angle) was chosen as the reference CC area. The mean cross-sectional CC

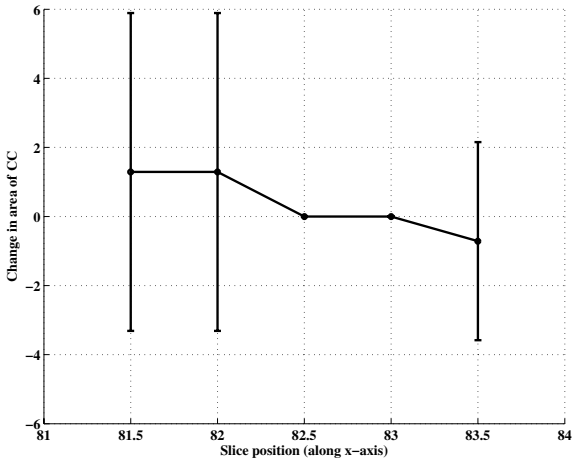

Fig. 7. Mean and standard deviation of percentage change (%) in CC area across the 15 MR volumes for nearest neighbor interpolation plotted against change in translation

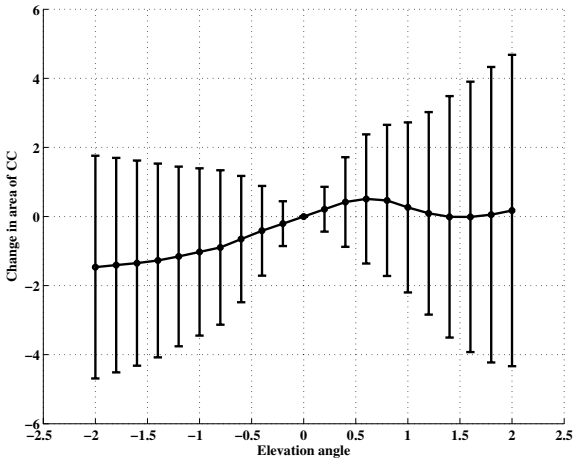

Fig. 9. Mean and standard deviation of percentage change (%) in CC area across the 15 MR volumes for trilinear interpolation plotted against change in elevation

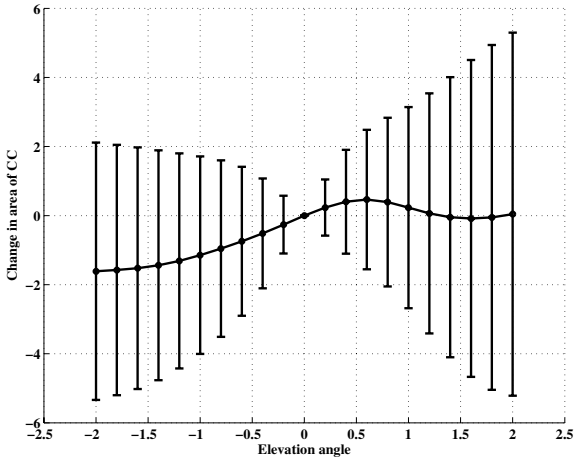

Fig. 8. Mean and standard deviation of percentage change (%) in CC area across the 15 MR volumes for tricubic interpolation plotted against change in elevation

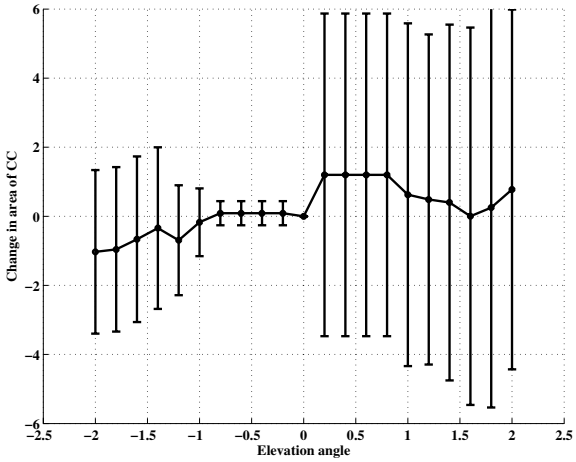

Fig. 10. Mean and standard deviation of percentage change (%) in CC area across the 15 MR volumes for nearest neighbor interpolation plotted against change in elevation

area change due to perturbation of the MSP was 2.67% with a median change of 1.98%, and a standard deviation 2.47%.

Figures 5–7 display the mean percentage change in cross-sectional CC area of the 15 MR volumes against the MSP translation range for tricubic, trilinear and nearest neighbor interpolations, respectively. The error bars represent the standard deviation of the change in cross-sectional CC areas among the 15 volumes at different slice positions with constant elevation and azimuth angles of 0 degrees.

Figures 8–10 display the mean percentage change in cross-sectional CC area against change in elevation angle from -2.0 degrees to 2.0 degrees for tricubic, trilinear and nearest neighbor interpolations, the error bars represent the standard deviation. The azimuth angle and slice position were kept constant at 0 degrees and 82.5, respectively.

Figures 11–13 display the mean percentage change in cross-sectional CC area against change in azimuth angle from -2.0 degrees to 2.0 degrees for tricubic, trilinear and nearest neighbor interpolations, with the error bars giving the standard deviation while the slice position and the elevation angle are kept constant at 82.5 and 0, respectively.

As stated above, the figures 5–13 represent the mean percentage change in cross-sectional CC areas and the standard deviations. However, these graphs do not display the maximum percentage change in CC areas. We show the CC areas with maximum changes in tables 1 to 4. The CC areas which have

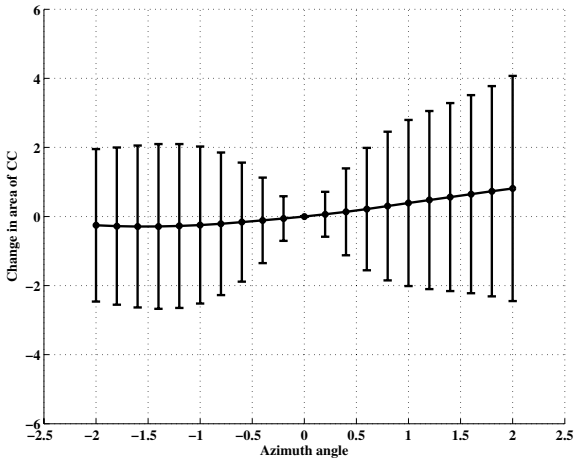

Fig. 11. Mean and standard deviation of percentage change (%) in CC area across the 15 MR volumes for tricubic interpolation plotted against change in azimuth

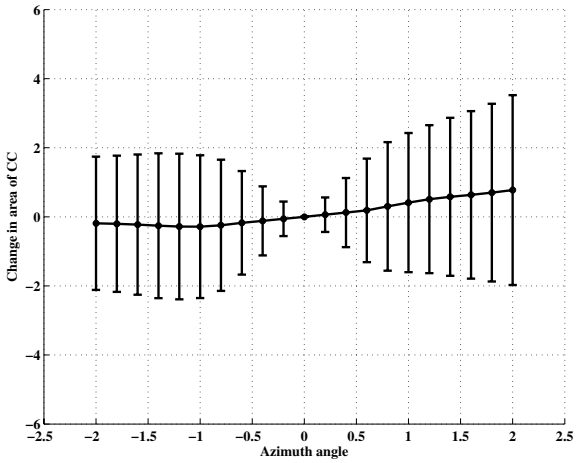

Fig. 12. Mean and standard deviation of percentage change (%) in CC area across the 15 MR volumes for trilinear interpolation plotted against change in azimuth

undergone the maximum change are shown as percentage of the reference CC area. Table 1 represent these extreme CC areas for change in translation, elevation angles and azimuth angles. Tables 2 and 3 isolate the extreme CC areas for elevation angles and azimuth angles, respectively. Table 4 displays the extreme values of CC areas for translation only while the elevation angles and the azimuth angles are kept constant at 0 degrees.

V. Conclusions

Our results emphasize the importance of the selection of both the MSP and the interpolation technique for the calculation of CC areas. Although the perturbation of MSP appears to

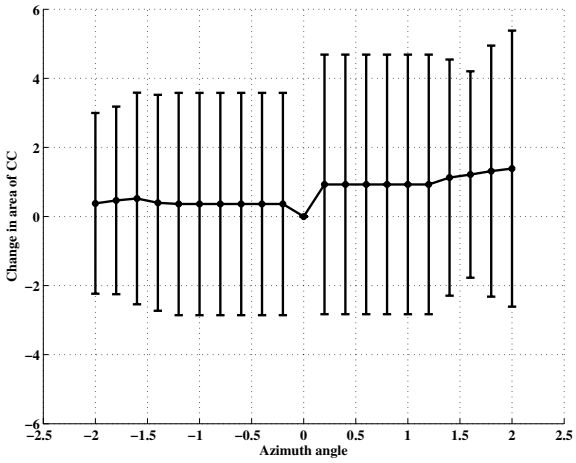

Fig. 13. Mean and standard deviation of percentage change (%) in CC area across the 15 MR volumes for nearest neighbor interpolation plotted against change in azimuth

Table 1. CC area with highest change as percentage of CC area in reference slice (elevation from -2 to 2 degrees, azimuth from -2 to 2 degrees)

Slice Position	Tricubic	Trilinear	Nearest
81.5	115.67	113.33	117.14
82.0	115.16	112.78	117.14
82.5	112.70	110.84	115.74
83.0	88.47	89.30	87.32
83.5	87.23	88.26	112.17

have a more profound influence on the calculated CC areas, yet it is clear that the choice of the interpolation technique also has a definite effect on the calculation. Since the goal of measuring CC areas for different pathologies is to isolate the effects of these pathologies on the CC, therefore any future study which focuses on CC area calculations must ensure that the error introduced due to MSP perturbation and image interpolation is minimized.

References

[1] A. Traboulsee, G. Zhao and D.K.B. Li, Neuroimaging in Multiple Sclerosis, Neurol Clin 23 (2005) 131148.
[2] G. Wideman Homepage, `http://www.grahamwideman.com/gw/brain/orientation/orientterms.htm`.

Table 2. CC area with highest change as percentage of CC area in reference slice (elevation from -2 to 2 degrees, azimuth = 0 degrees)

Slice Position	Tricubic	Trilinear	Nearest
81.5	114.95	112.61	87.18
82.0	114.88	112.41	87.18
82.5	112.66	110.84	85.57
83.0	89.23	89.84	111.15
83.5	89.30	89.75	110.28

Table 3. CC area with highest change as percentage of CC area in reference slice (elevation = 0 degrees, azimuth from -2 to 2 degrees)

Slice Position	Tricubic	Trilinear	Nearest
81.5	110.97	109.76	116.89
82.0	108.63	107.34	112.02
82.5	109.55	108.00	109.59
83.0	108.98	107.51	110.91
83.5	91.44	92.12	107.96

Table 4. CC area with highest change as percentage of CC area in reference slice (elevation = 0 degrees, azimuth = 0 degrees)

Slice Position	Tricubic	Trilinear	Nearest
81.5	92.00	93.49	111.15
82.0	105.01	105.28	111.15
82.5	100.00	100.00	100.00
83.0	94.26	94.71	100.00
83.5	91.78	92.80	94.73

[3] K.V. Skoglund, M.B. Stegmann, C. Ryberg, H. lafsdttir1 and E. Rostrup, Estimation and Perturbation of the Mid-Sagittal Plane and its Effects on Corpus Callosum Morphometry, ISMRM, 2005.

[4] A. Kutzelnigg, C.F. Lucchinetti, C. Stadelmann, W.Bruck, H. Rauschka, M. Bergmann, M. Schmidbauer, J.E. Parisi and H. Lassmann, Cortical demyelination and diffuse white matter injury in multiple sclerosis, Brain (2005), Vol 128, pp. 27052712.

[5] Multiple sclerosis society of Canada homepage, `http://www.mssociety.ca`.

[6] NINDS Multiple Sclerosis Information Page, `http://www.ninds.nih.gov/disorders/multiple_sclerosis/multiple_sclerosis.htm`.

[7] J.L. Ostuni, A.K.S. Santha, V.S. Mattay, D.R. Weinberger, R.L. Levin and J.A. Frank, Analysis of interpolation effects in the reslicing of functional MR-images, J. Computer Assisted Tomography, vol. 21, no. 5, pp. 803-810, 1997.

[8] H.W. Venema, S.S.K.S. Phoa, P.G.B. Mirck, F.J.H. Hulsmans, C.B.L.M. Majoie and B. Verbeeten Jr, Petrosal Bone: Coronal Reconstructions from Axial Spiral CT Data Obtained with 0.5-mm Collimation Can Replace Direct Coronal Sequential CT Scans, Radiology, 1999 Nov, 213(2) 375-82.

[9] C. Ryberg, M. B. Stegmann, K. Sjstrand, E. Rostrup, F. Barkhof, F. Fazekas, G. Waldemar, Corpus Callosum Partitioning Schemes and Their Effect on Callosal Morphometry, Proc. International Society of Magnetic Resonance In Medicine - ISMRM 2006, Seattle, Washington, USA.

[10] M. B. Stegmann, K. Skoglund, On Automating and Standardising Corpus Callosum Analysis in Brain MRI, Proc. Svenska Symposium i Bildanalys, SSBA 2005, Malm, Sweden, pp. 1-4, SSBA, 2005.

[11] M. B. Stegmann, K. Skoglund, C. Ryberg, Mid-sagittal plane and mid-sagittal surface optimization in brain MRI using a local symmetry measure, International Symposium on Medical Imaging 2005, San Diego, CA, Proc. of SPIE, vol. 5747, pp. 568-579, SPIE, 2005.

[12] M. Kass, A. Witkin, and D. Terzopoulos, Snakes - Active Contour Models, International Journal of Computer Vision, 1(4): 321-331, 1987.

[13] R. Malladi, J. A. Sethian, B. C. Vemuri, Shape modeling with front propagation: A level set approach, IEEE Transactions on Pattern Analysis and Machine Intelligence, 17(2): 158-175, Feburary 1995.

[14] M. B. Stegmann, The AAM-API: An Open Source Active Appearance Model Implementation, Medical Image Computing and Computer-Assisted Intervention - MICCAI 2003, 6th Int. Conference, Montral, Canada, pp. 951-952.

[15] S. Kichenassamy, A. Kumar, P. Olver, A. Tannenbaum, A. Yezzi, Gradient flows and geometric active contour models, iccv, p. 810, Fifth International Conference on Computer Vision (ICCV'95), 1995.

[16] M.E. Leventon, W.E.L. Grimson, O. Faugeras, W.M.W. Iii, Level Set Based Segmentation with Intensity and Curvature Priors, mmbia, p. 4, IEEE Workshop on Mathematical Methods in Biomedical Image Analysis (MMBIA'00), 2000.